Supplementary Tables and Figures

Type 1 conventional dendritic cells and interferons are required for spontaneous CD4$^+$ and CD8$^+$ T cell protective responses to breast cancer

Raphaël Mattiuz, Carine Brousse, Marc Ambrosini, Jean-Charles Cancel, Gilles Bessou, Julie Mussard, Amélien Sanlaville, Christophe Caux, Nathalie Bendriss-Vermare, Jenny Valladeau-Guilemond, Marc Dalod, Karine Crozat

Supplementary table 1. Mouse strains used in this study

Type	Mouse strains[1]	Official nomenclatures	References[2]	Source
KI	*Karma-tmt-hDTR*	*Gpr141b$^{tm1(HBEGF)Ciphe}$*	1	Dalod lab/Ciphe
	Tg^{TcraTcrb1100Mjb}; Rag2$^{-/-}$	C57BL/6-Tg(TcraTcrb)1100Mjb/J; B6(Cg)-*Rag2$^{tm1.1Cgn}$*/J	2, 3	CIML: Dr. A.M. Schmidt-Verhulst Jackson Laboratory (Stock n° 003831; 008449)
	Ubc-GFP$^{+/+}$	C57BL/6-Tg(UBC-GFP)30Scha/J	4	CIML: Dr. M. Bajénoff Jackson Laboratory (Stock n° 004353)
KO	*Ccr7$^{-/-}$*	B6.129P2(C)-*Ccr7^{tm1Rfor}*/J	5	CIML: Dr. H. Lelouard Jackson Laboratory (Stock n° 006621)
	Cxcl9$^{-/-}$	B6-*Cxcl9^{tm2Ciphe}*	This paper	Dalod lab/Ciphe
	Ifnar1$^{-/-}$	B6.129S2-*Ifnar1^{tm1Agt}*	6, 7	Pr. U. Kalinke
	Ifngr1$^{-/-}$	B6.129S7-*Ifngr1^{tm1Agt}*/J	8	CIML: Dr. H. Lelouard Jackson Laboratory (Stock n° 003288)
	Il12b$^{-/-}$	B6.129S1-*Il12b^{tm1Jm}*/J	9	CIML: Dr. H. Lelouard Jackson Laboratory (Stock n° 002693)
	Il15ra$^{-/-}$	B6;129X1-*Il15ra^{tm1Ama}*/J	10	Jackson Laboratory (Stock n° 003723)
	Stat1$^{-/-}$	*B6-Stat1$^{tm1d(EUCOMM)Ciphe}$*	11	EUCOMM/ Dalod lab/Ciphe
	Xcr1$^{-/-}$	B6.129P2-*Xcr1^{tm1Dgen}*/J	12, 13	Jackson Laboratory (Stock n° 005791)
Cre	*Karma^{Cre}*	B6-*Gpr141b^{tm2Ciphe}*	14	Dalod lab/Ciphe
	Xcr1^{Cre}	B6-*Xcr1^{tm1Ciphe}*	14	Dalod lab/Ciphe
Floxed	*Cxcl9^{fl}*	B6-*Cxcl9^{tm1Ciphe}*	This paper	Dalod lab/Ciphe
	Ifnar1^{fl}	*Ifnar1^{tm1Uka}*	15, 16	Pr. U. Kalinke
	Il15ra^{fl}	C57BL/6-*Il15ra$^{tm2.1Ama}$*/J	17	Jackson Laboratory (Stock n° 022365)
	Rosa26$^{lox-stop-lox-DTA}$	B6.129P2-*Gt(ROSA)26Sor$^{tm1(DTA)Lky}$*/J	18	Prs. D. Voehringer & R.M. Locksley Jackson Laboratory (Stock n° 009669)
	Rosa26$^{lox-stop-lox-hDTR}$	*Gt(ROSA)26Sor$^{tm1(HBEGF)Awai}$*/J	19	CIML: Dr. M. Sieweke Jackson Laboratory (Stock n° 007900)
	Rosa26$^{lox-stop-lox-tdRFP}$	*Gt(ROSA)26Sor^{tm1Hjf}*	20	CIML: Dr. H. Luche

[1]All mice were maintained in a C57BL/6J background.
[2]References, see at the end of this supplementary file.

Supplementary table 2. Antibodies used in this study

Antibody	Clone	Conjugates	Company	Dilution/Dose	Use
Arm Hamster	Polyclonal	A594	Jackson ImmunoResearch	1/200	Microscopy
CD3ε	145-2C11	BV510	BD Biosciences	1/200	Flow cytometry
CD3ε	145-2C11	Purified	BD Biosciences	1/300	Flow cytometry
CD4	GK1.5	Purified	BioXCell	500 µg	*In vivo* depletion
CD4	GK1.5	APC-H7	BD Biosciences	1/200	Flow cytometry
CD4	RM4-5	ef450	ThermoFisher Scientific	1/100	Microscopy
CD8α	53-6.7	PerCP-Cy5.5	BD Biosciences	1/200	Flow cytometry
CD8β	H35-17.2	Purified	produced_in_house	150 µg	*In vivo* depletion
CD11b	M1/70	BUV395	BD Biosciences	1/400	Flow cytometry
CD11c	N418	BV785	BioLegend	1/200	Flow cytometry
CD19	1D3	BV510	BD Biosciences	1/200	Flow cytometry
CD19	1D3	Alexa700	BD Biosciences	1/200	Flow cytometry
CD24	M1/69	eFluor450	eBioscience	1/1000	Flow cytometry
CD25	PC61	BV421	BD Biosciences	1/600	Flow cytometry
CD40	3/23	PE	BD Biosciences	1/200	Flow cytometry
CD43	1B11[1]	PE-Cy5	BioLegend	1/200	Flow cytometry
CD44	IM7	PE-Cy7	eBioscience	1/800	Flow cytometry
CD45.2	104	V500	BD Biosciences	1/200	Flow cytometry
CD45.2	104	BUV737	BD Biosciences	1/400	Flow cytometry
CD62l	MEL-14	BV421	BD Biosciences	1/400	Flow cytometry
CD64	X54-5/7.1	BV711	BioLegend	1/200	Flow cytometry
CD69	H1.2F3	FITC	eBioscience	1/200	Flow cytometry
CD80	16-10A1	APC	BD Biosciences	1/200	Flow cytometry
CD86	GL1	PE-Cy7	BD Biosciences	1/400	Flow cytometry
CD117	2B8	PE-Cy7	BD Biosciences	1/200	Flow cytometry
CD172a	P84	FITC	BD Biosciences	1/200	Flow cytometry
CCR7	4B12	Biotin	eBioscience	1/100	Flow cytometry
CCR7	4B12	PE	BD Biosciences	1/100	Flow cytometry
CTLA-4	9D9	Purified	BioXCell	200 µg	*In vivo* depletion
F4/80	BM8	BV605	BioLegend	1/200	Flow cytometry
FcεRIα	MAR-1	PacificBlue	BioLegend	1/200	Flow cytometry
FoxP3	FJK-16s	Biotin	eBioscience	1/100	Flow cytometry
GFP	Polyclonal (Rabbit)	A488	Invitrogen	1/1000	Microscopy
GzmB	GB11	APC	Invitrogen	1/100	Flow cytometry
HER2	7.16.4	Purified	BioXCell	1/1000	Microscopy
IFNγ	XMG1.2	Alexa700	BD Biosciences	1/200	Flow cytometry
Ki67	B56	V450	BD Biosciences	1/100	Flow cytometry
LAG3	C9B7W	BV711	BD Biosciences	1/200	Flow cytometry
Ly-6C	AL-21	APC-Cy7	BD Biosciences	1/1000	Flow cytometry
MHC-II	M5/114.15.2	Alexa700	BioLegend	1/400	Flow cytometry
NK1.1	PK136	Purified	produced_in_house	200 µg	*In vivo* depletion
NK1.1	PK136	BV650	BioLegend	1/400	Flow cytometry
NKp46	29A1.4	BV510	BD Biosciences	1/200	Flow cytometry
PD-1	29F.1A12	BV785	BioLegend	1/400	Flow cytometry
Rabbit	Polyclonal (Donkey)	A647	Molecular Probes	1/500	Microscopy
RFP	Polyclonal (Rabbit)	Purified	Rockland	1/500	Microscopy
Siglec-H	551	PerCP-Cy5.5	BioLegend	1/200	Flow cytometry
TCRβ	H57-597	FITC	BD Biosciences	1/200	Flow cytometry
Tim-3	RMT3-23	BV605	BioLegend	1/200	Flow cytometry
TNFα	MP6-XT22	BV785	BioLegend	1/200	Flow cytometry
XCR1	ZET	BV650	BioLegend	1/1000	Flow cytometry

[1]The 1B11 clone of anti-CD43 mAb recognizes the glycosylated isoform of the molecule that is specifically expressed on effector T cells, in particular effector $CD8^+$ T cells endowed with cytotoxic activity[21].

Supplementary table 3. Primers used in this study for qRT-PCR

	Forward primers	Reverse primers
Hprt	5′-GGCCCTCTGTGTGCTCAAG-3′	5′-CTGATAAAATCTACAGTCATAGGAATGGA-3′
Ifna2	5'-AGGACAGGCAGGACTTTGGA-3'	5'-GCCTTCTGGATCTGCTGGTTA-3'
Ifna4	5'-AAGGACAGGAAGGATTTTGGATT-3'	5'-GAGCCTTCTGGATCTGTTGGTT-3'
Ifnb	5'-GGTGGTCCGAGCAGATCTT-3'	5'-CAGTTTTGGAAGTTTCTGGTAAGTCTT-3'
Ifng	5'-CAACAGCAAGGCGAAAAAGG-3'	5'-CCTGTGGGTTGTTGACCTCAA-3'
Irf7	5′-TCCAGTTGATCCGCATAAGGT-3′	5′-CTTCCCTATTTTCCGTGGCTG-3′
Isg15	5′-GGTGTCCGTGACTAACTCCAT-3′	5′-TGGAAAGGGTAAGACCGTCCT-3′
Mx1	5'-GACCATAGGGGTCTTGACCAA-3'	5'-AGACTTGCTCTTTCTGAAAAGCC-3'
Oas3	5'-TCTGGGGTCGCTAAACATCAC-3'	5'-GATGACGAGTTCGACATCGGT-3'

Supplementary Figure 1

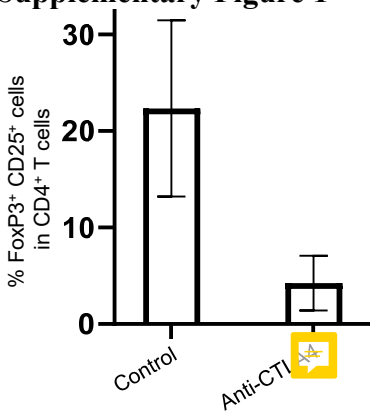

Supplementary Figure 1. Efficacy of the depletion of regulatory $CD4^+$ T cells in NOP23 tumors.

Mice were administered anti-CTLA-4 mAb (clone 9D9, 200 µg per injection) 1d before NOP23 cell engraftment, then every three days. Mice were euthanized at day 7 and tumors were harvested for analysis of their content in regulatory $CD4^+$ T cells by flow cytometry, defined as the percent of $Foxp3^+$ $CD25^+$ cells within singlet, non-autofluorescent $CD45.2^+$ $CD19^-$ $TCR\beta^+$ $CD8\alpha^-$ $CD4^+$ T lymphocytes.
Data are shown as mean±SEM. n=3 for anti-CTLA-4-treated mice, n=2 for control mice.

Supplementary Figure 2

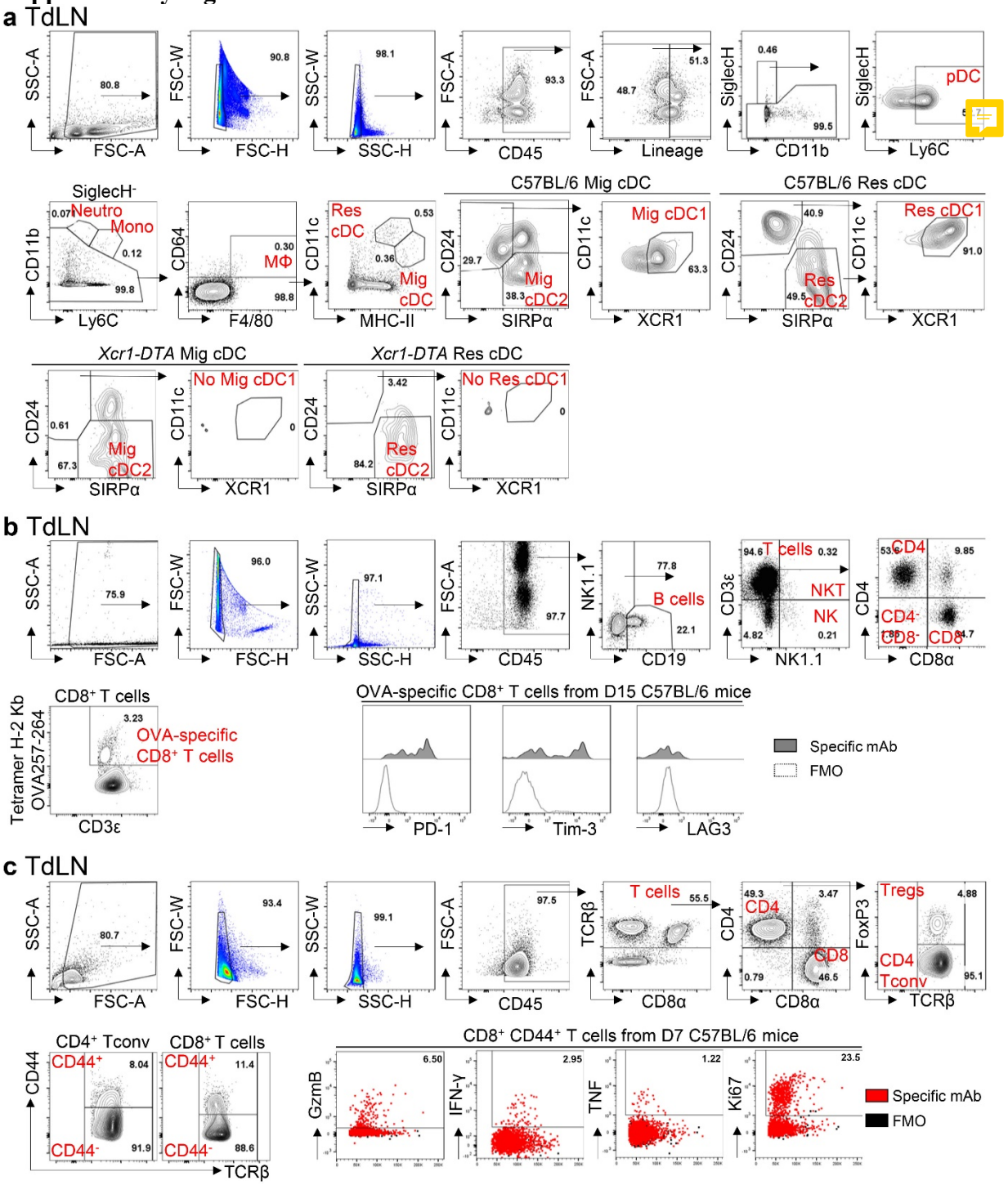

Supplementary Figure 2. Gating strategies used to identify myeloid and lymphoid cell populations in TdLNs of *Wt*, *Ifnar1*$^{-/-}$, *Ifngr1*$^{-/-}$ and *Xcr1-DTA* mice, used in Fig.2, Fig.5, Fig.7, Supplementary Fig. 6 and Supplementary Fig. 8.

One sample at d7 post-tumor engraftment is shown as representative of all samples. Data are shown for one experiment representative of two. Lineage (CD19, CD3ε and NKp46) exclusion is used in myeloid gating strategy (**a**). This figure also includes: the depletion of Migratory and Resident cDC1 in *Xcr1-DTA* (**a**); the expression of PD-1, Tim-3 and LAG3 in OVA-specific CD8^{+} T cells in *Wt* mice at d15 post tumor engraftment (**b**, bottom); and GzmB, IFN-γ, TNF and Ki67 expression in CD44^{+} CD8^{+} T cells in *Wt* mice at D7 post tumor engraftment after *ex-vivo* SIINFEKL peptide re-stimulation (**c**, bottom).

Supplementary Figure 3

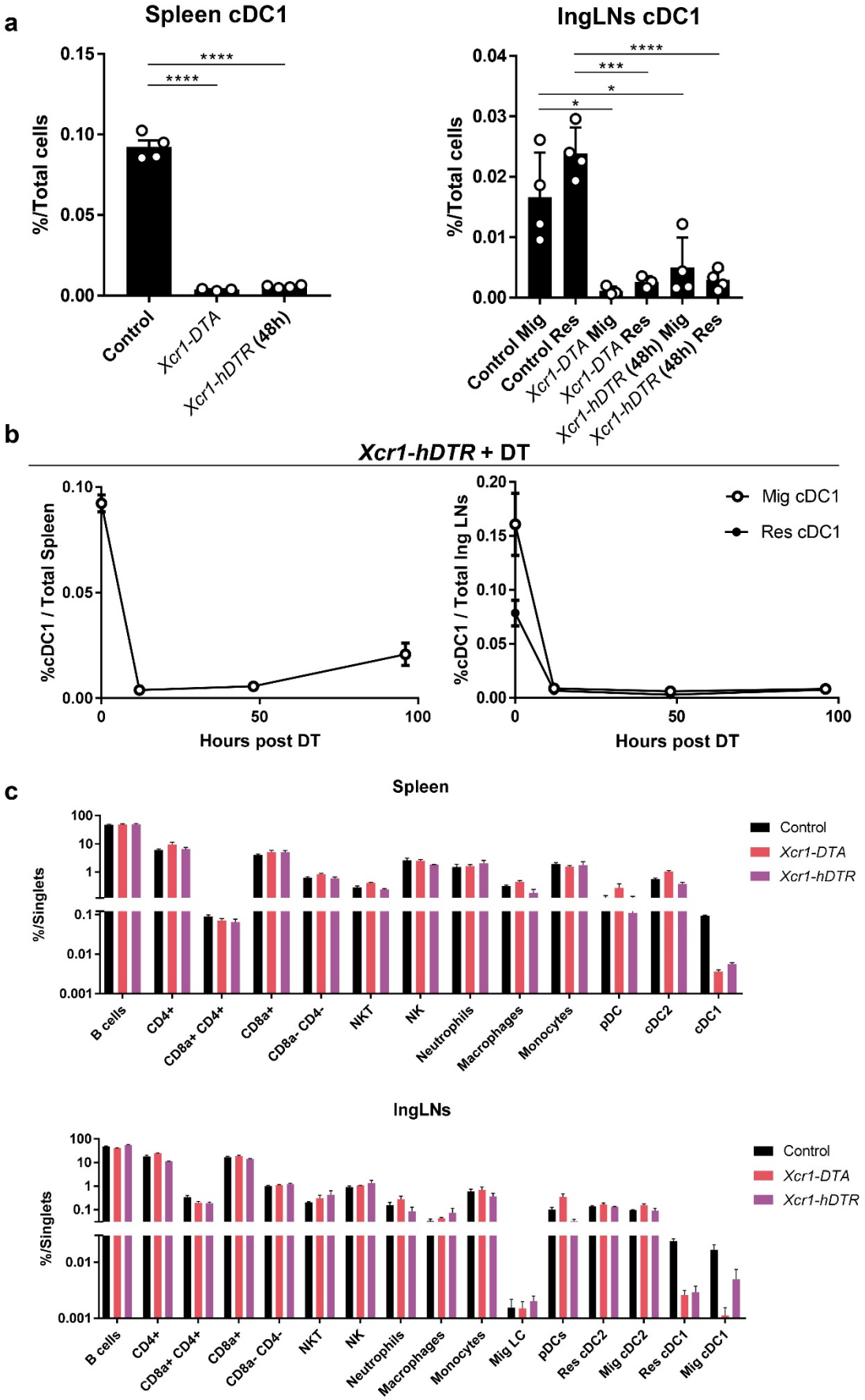

Supplementary Figure 3. Efficient cDC1 depletion in *Xcr1-DTA* and *Xcr1-hDTR* mice.

(**a**) cDC1 proportion in spleen (left) and IngLNs (right) in *Xcr1-DTA* and *Xcr1-hDTR* mice (48h after DT). Data are shown as one dot per mouse with mean±SEM per group. (**b**) Kinetics of cDC1 depletion

in spleen (left) and IngLNs (right) after one DT injection in *Xcr1-hDTR* mice. Data are shown as mean±SEM. (**c**) %/total cells (mean±SEM) for the indicated populations in spleen (top) and IngLNs (bottom) in *Xcr1-DTA*, *Xcr1-hDTR* (48h after DT) and control mice. The data shown are for 3-4 mice per condition from one experiment representative of two independent ones. *, $P < 0.05$; **, $P < 0.01$; ***, $P < 0.001$; ****, $P < 0.0001$ (unpaired *t*-test).

Supplementary Figure 4.

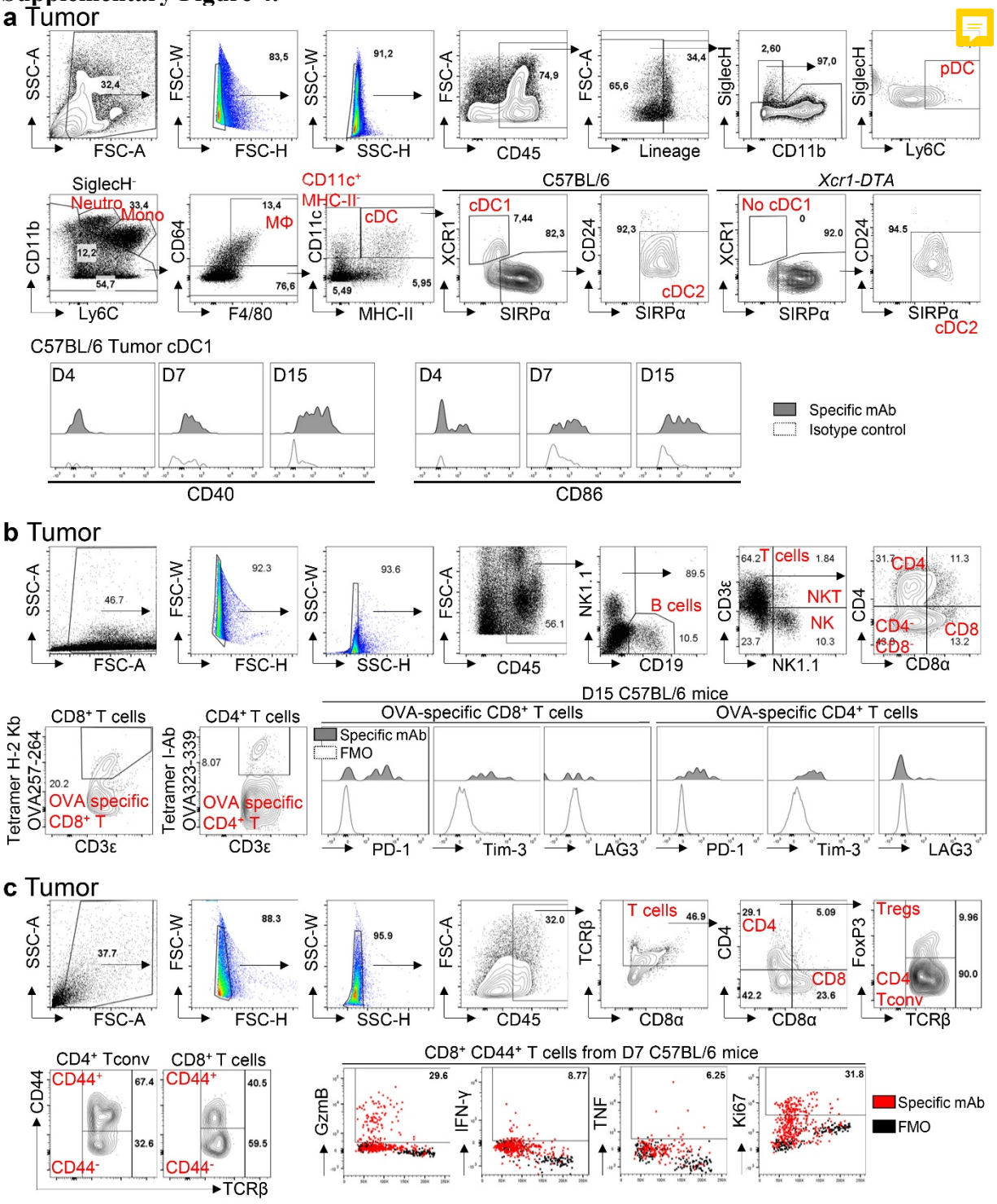

Supplementary Figure 4. Gating strategies used to identify myeloid and lymphoid cell populations in tumors of *Wt*, *Ifnar1*$^{-/-}$, *Ifngr1*$^{-/-}$ and *Xcr1-DTA* mice, used in Fig.5, Fig.6, Fig.7, Supplementary Fig. 7, Supplementary Fig. 8 and Supplementary Fig. 10.

One sample at d7 post tumor engraftment is shown as representative of all samples. Data are shown for one experiment representative of two. Lineage (CD19, CD3ε and NKp46) exclusion is used in myeloid gating strategy (**a**). This figure also includes: the depletion of tumor cDC1 in *Xcr1-DTA* (**a**, top); the expression of CD40 and CD86 in cDC1 in *Wt* mice at d4, d7 and d15 post engraftment (**a**, bottom); the expression of PD-1, Tim-3 and LAG3 in OVA-specific $CD4^+$ and $CD8^+$ T cells in *Wt* mice at d15 post tumor engraftment (**b**, bottom); and GzmB, IFN-γ, TNF and Ki67 expression in $CD44^+$ $CD8^+$ T cells in *Wt* mice at d7 post tumor engraftment after *ex-vivo* SIINFEKL peptide re-stimulation (**c**, bottom).

Supplementary Figure 5

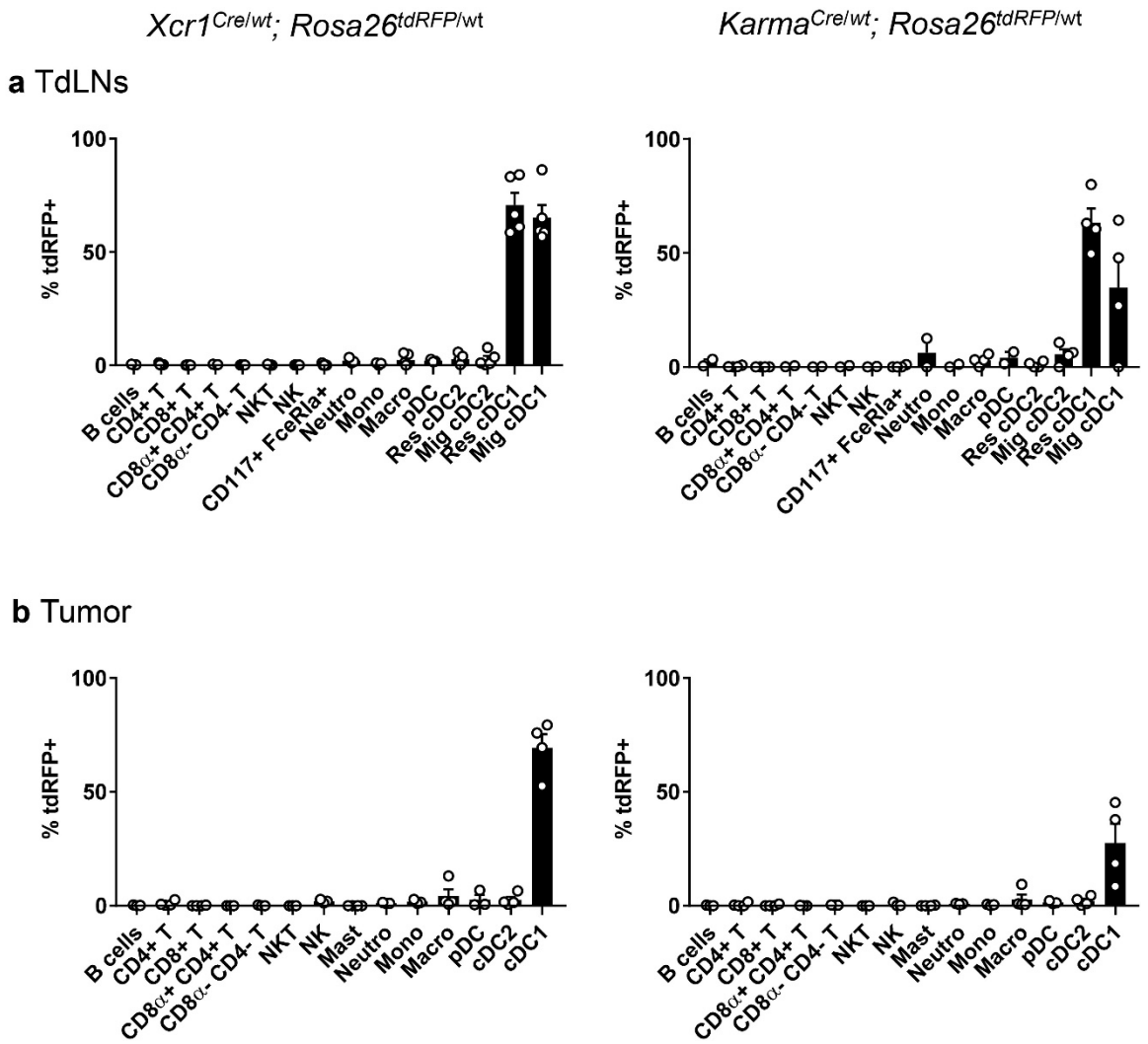

Supplementary Figure 5. The *Xcr1*$^{Cre/wt}$*;Rosa26*$^{tdRFP/wt}$ and *Karma*$^{Cre/wt}$*;Rosa26*$^{tdRFP/wt}$ mouse strains allow specific fate mapping of cDC1 in the tumor and TdLNs.

tdRFP expression analysis by different immune cell populations from TdLNs (**a**) and tumors (**b**) at d4 post engraftment in *Xcr1*$^{Cre/wt}$*;Rosa26*$^{tdRFP/wt}$ and *Karma*$^{Cre/wt}$*;Rosa26*$^{tdRFP/wt}$ mice. The data shown (one dot per mouse with mean±SEM per group) are from two independent experiments pooled together.

Supplementary Figure 6

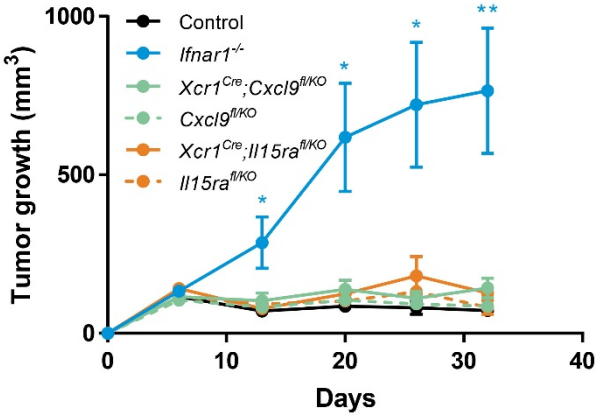

Supplementary Figure 6. CXCL9 production and IL-15 trans-presentation by cDC1 are not necessary for tumor rejection.

Tumor growth (mean±SEM) in *Ifnar1*$^{-/-}$ (n=7), *Xcr1*^{cre}*;Cxcl9*$^{fl/KO}$ (n=4), *Cxcl9*$^{fl/KO}$ (n=6), *Xcr1*^{cre}*;Il15ra*$^{fl/KO}$ (n=4) and *Il15ra*$^{fl/KO}$ (n=5) and Control (n=6) female mice. One experiment representative of >2 independent ones is shown. *, $P < 0.05$; **, $P < 0.01$; ***, $P < 0.001$ (unpaired *t*-test).

Supplementary Figure 7

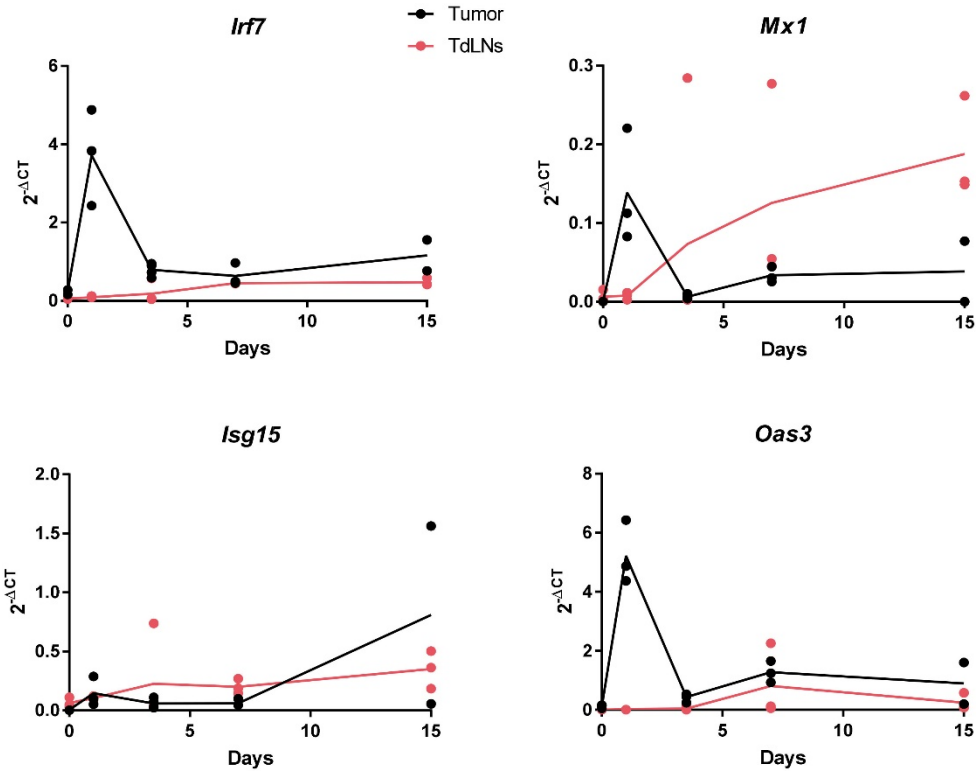

Supplementary Figure 7. ISGs are transcribed in tumor and TdLNs.

Expression of the *Irf7*, *Mx1*, *Isg15* and *Oas3* genes overtime in tumor and TdLNs (n=2-4) from *WT* mice.

Supplementary Figure 8

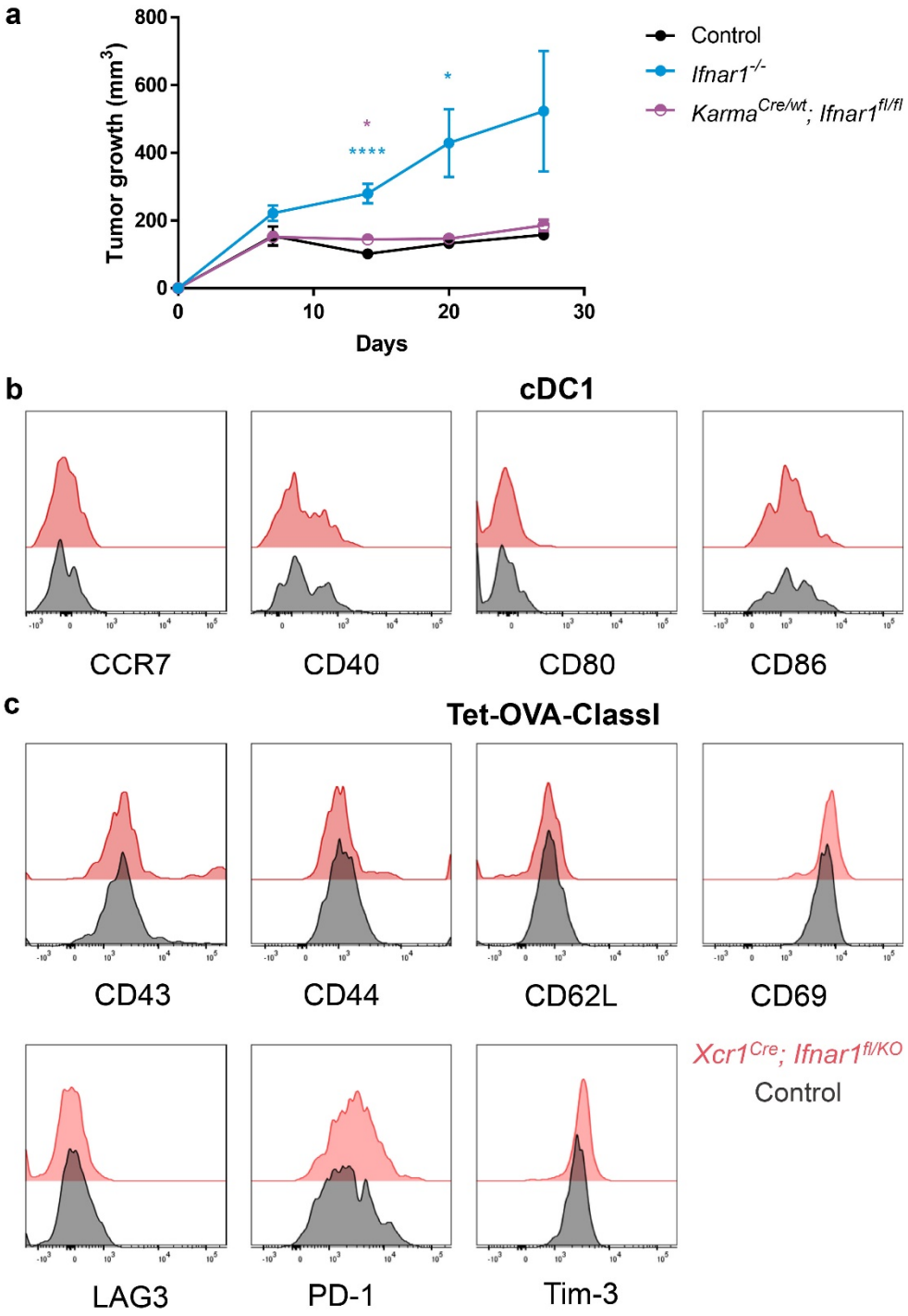

Supplementary Figure 8. cDC1 cell-intrinsic responses to IFN-I are dispensable for tumor control. (**a**) Tumor growth (mean±SEM) in *Ifnar1*$^{-/-}$ (n=8), *Karma*$^{Cre/wt}$*;Ifnar1*$^{fl/fl}$ (n=8) and control (n=7) female mice. One experiment representative of two independent ones is shown. *, P <0.05; **, P<0.01; ***, P<0.001; ****, P<0.0001 (unpaired t-test). (**b-c)** Expression of activation markers on tumor-infiltrating cDC1 (**b**) and Ag-specific CD8^{+} T cells (**c**) at d25 post-engraftment in *Xcr1*^{cre}*;Ifnar1*$^{fl/KO}$ and control mice.

Supplementary Figure 9

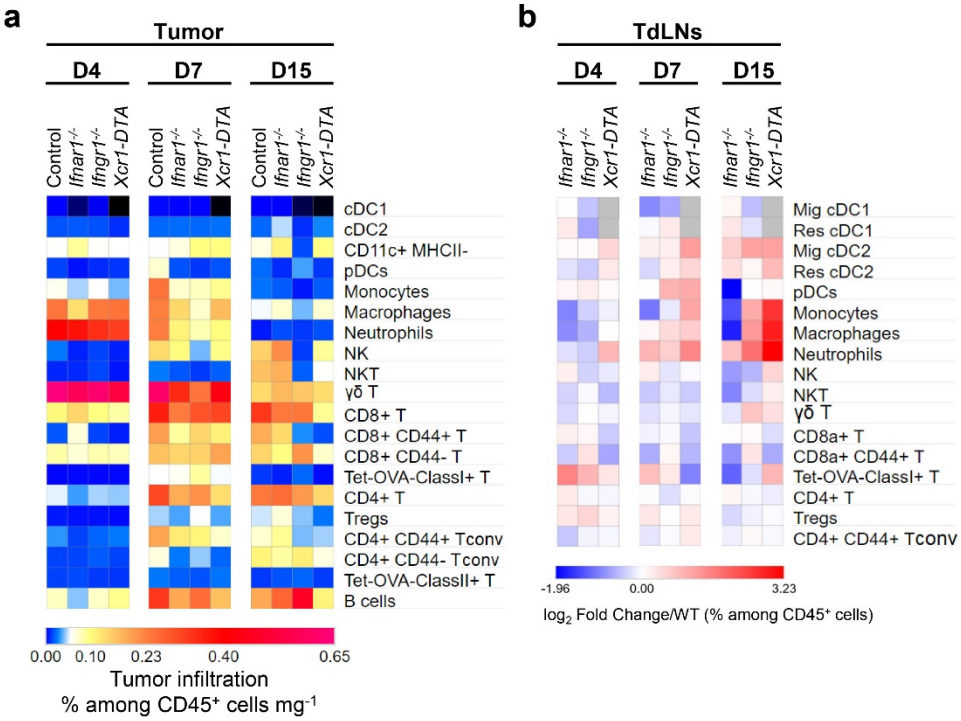

Supplementary Figure 9. cDC1 and IFN signaling shape the tumor immune landscape.

Heatmaps representing the global immune landscapes in the tumors (**a**) and TdLNs (**a**) at d4, d7 and d15 after engraftment in *Ifnar1*$^{-/-}$, *Ifngr1*$^{-/-}$, *Xcr1-DTA* and control mice (n=3-6 mice per group). The data are shown as (mean % Population/CD45^{+}/mg) (**a**) and as $\log_2$ Fold Changes calculated as the ratio of % Population/CD45^{+} from mutant animals to WT (b). The data shown are from two independent experiments pooled together.

Supplementary Figure 10

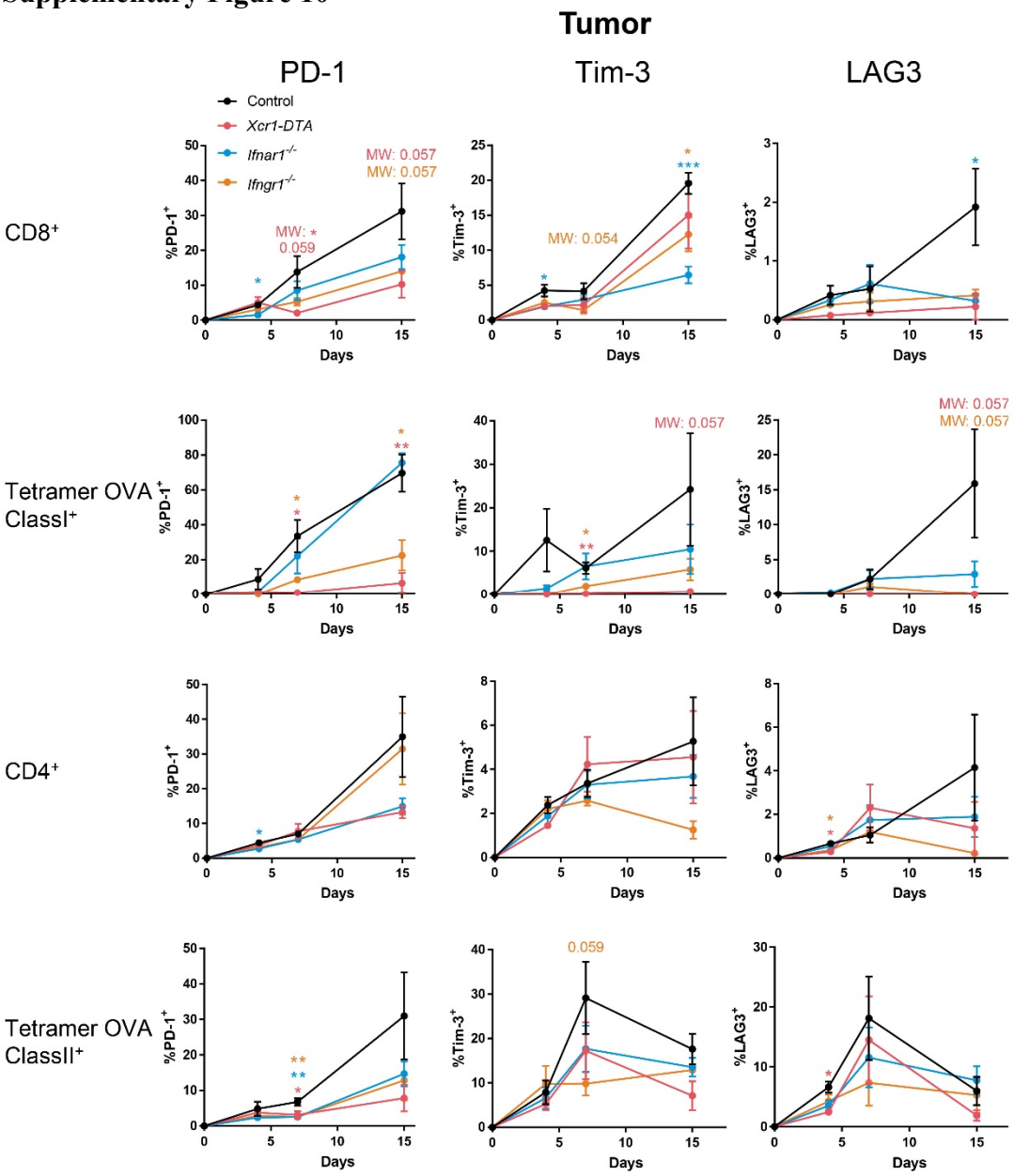

Supplementary Figure 10. cDC1, IFN-I and IFN-γ signaling are necessary for $CD4^+$ and $CD8^+$ T cell terminal activation in the TME.

Frequencies of $PD\text{-}1^+$; $Tim\text{-}3^+$ and $LAG3^+$ among $CD8^+$, Ag-specific $CD8^+$, $CD4^+$ and Ag-specific $CD4^+$ T cells at d4, d7 and d15 in the tumors from control, *Ifnar1*$^{-/-}$, *Ifngr1*$^{-/-}$ and *Xcr1-DTA* mice. The data shown (mean±SEM) are from two independent experiments pooled together (n=3-6 mice per group). ns, not significant ($P>0.05$); *, $P<0.05$; **, $P<0.01$; ***, $P<0.001$; (unpaired *t*-test or nonparametric Mann-Whitney *U*-test [MW] when specified).

Supplementary Figure 11

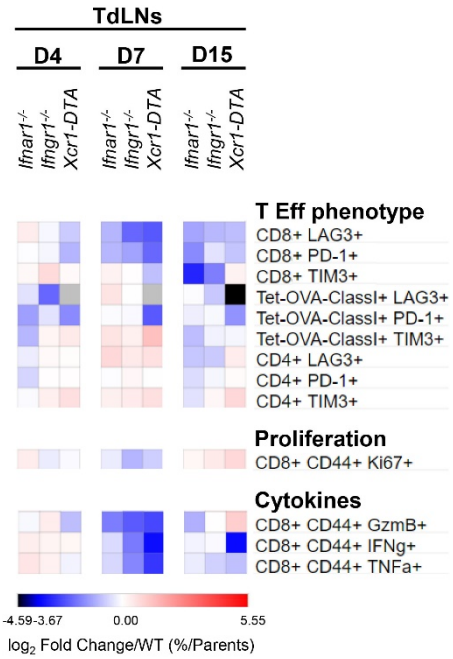

Supplementary Figure 11. cDC1, IFN-I and IFN-γ signaling shape TdLN immune composition, immune population activation states and effector functions.

Heatmap representing effector T cell phenotype, CTL proliferation and CTL cytokine production. For cytokine production, cell suspensions were restimulated *ex vivo* with SIINFEKL peptide. The data are shown as log_2 Fold Changes of the mean %Population/Parent population of mutant animals compared to their WT counterparts (n=3-6 mice per group). The data shown are from two independent experiments pooled together.

Supplementary Figure 12

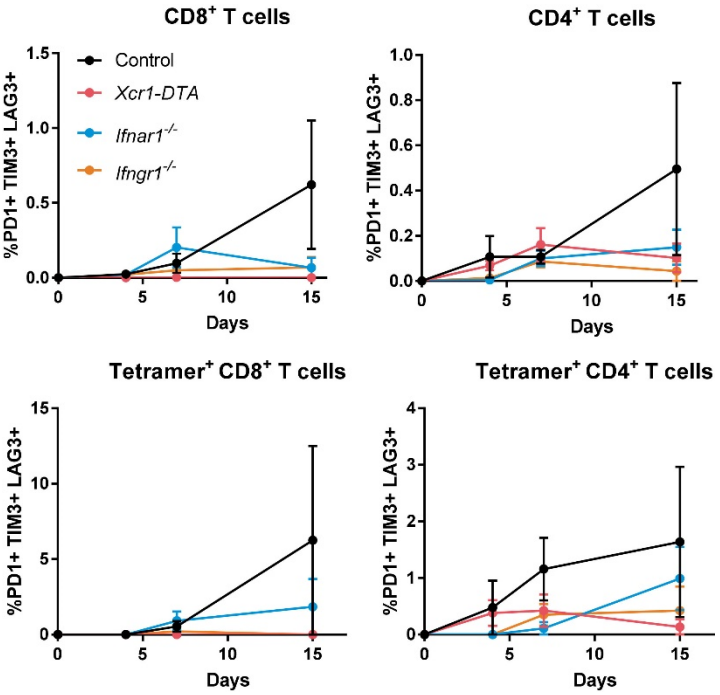

Supplementary Figure 12. "Exhausted-like" T cells are rare in tumors.

Kinetic analysis of the percent of tumor-infiltrating cells co-expressing PD-1, Tim-3 and LAG3 among $CD8^+$, Ag-specific $CD8^+$, $CD4^+$ and Ag-specific $CD4^+$ T cells at d4, d7 and d15 in *Ifnar1*$^{-/-}$, *Ifngr1*$^{-/-}$ and *Xcr1-DTA* and in control mice. The data shown (mean±SEM) are from two independent experiments pooled together, each with 3-6 mice per experimental group.

Supplementary Figure 13

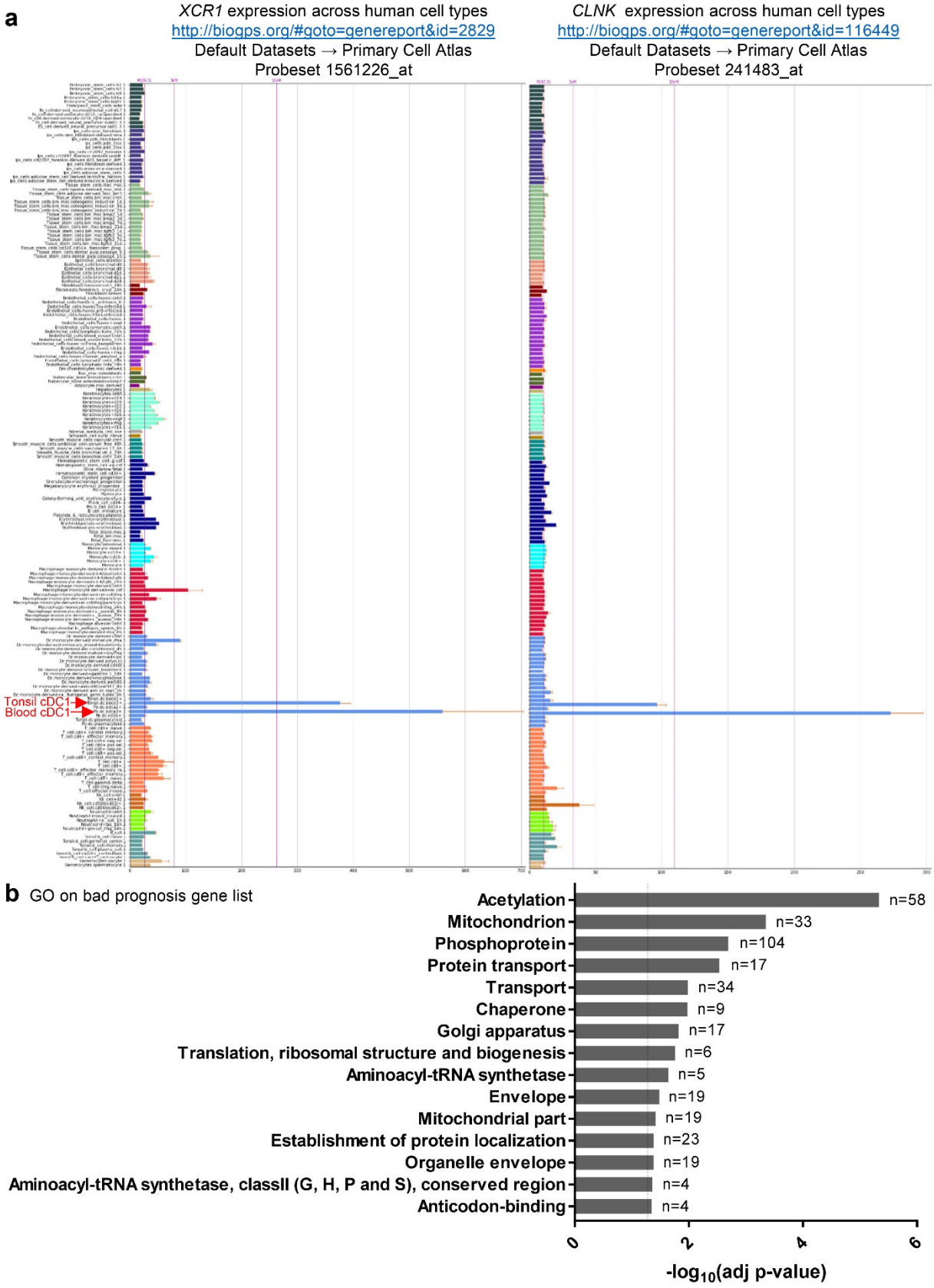

Supplementary Figure 13. Expression pattern of cDC1 signature genes across human cell types, and gene ontology analysis of genes associated with a bad prognosis in human breast cancer patients.

(**a**) Expression pattern of the *XCR1* and *CLNK* genes across a variety of human cell types. (**b**) Gene Ontology of the breast cancer bad prognosis gene set showing its association with an active metabolism. The data source used and the type of analysis performed are the same as depicted in the legend of Figure 8.

Supplementary Figure 14

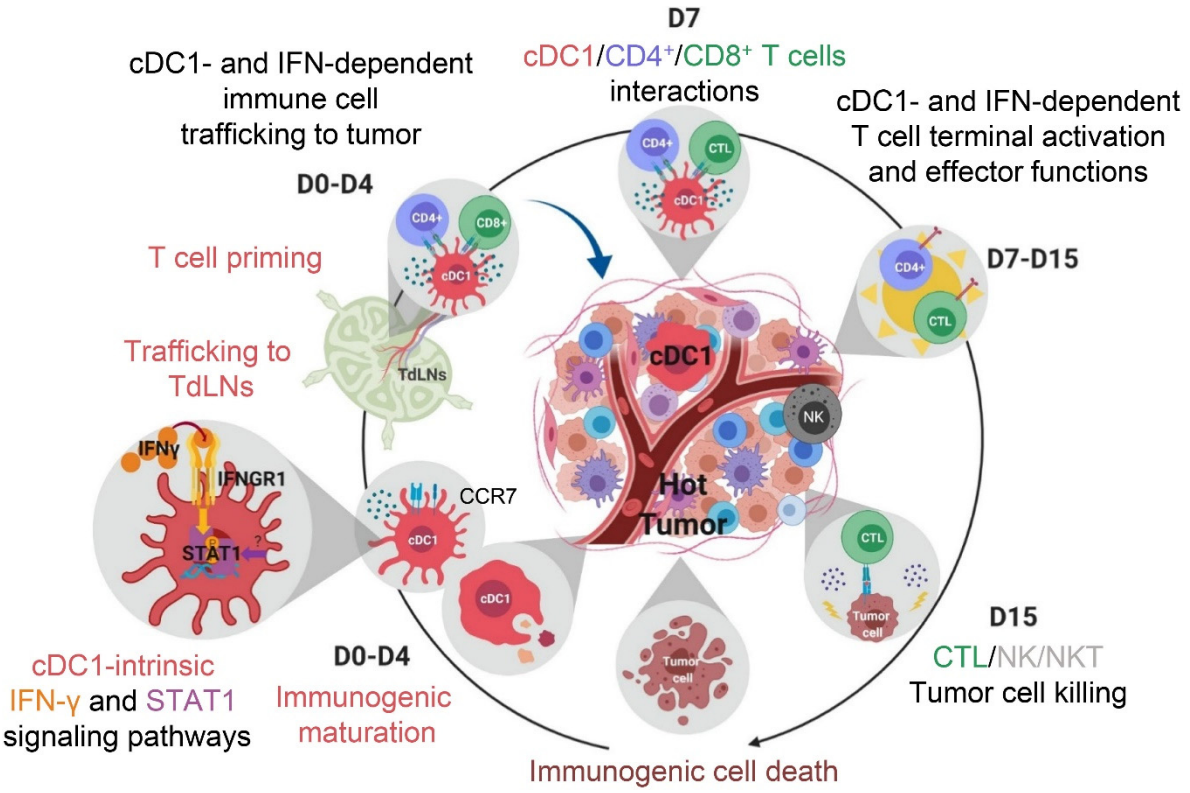

Supplementary Figure 14. Proposed model of cDC1 and IFN role in the immunosurveillance against breast cancer.

Within the 4 first days after tumor engraftment, type I IFNs and IFN-γ participate in shaping a microenvironment suitable to confer immunogenicity to cDC1 resident of tumors, or in the periphery of tumors. These cDC1 acquire CCR7 expression, which confers them their capacity to migrate into the TdLN. In the TdLN, they may prime both $CD4^+$ and $CD8^+$ T cells in type I IFN-independent manner. At day 7 in the TME, cDC1 are seen interacting simultaneously with $CD4^+$ and tumor-specific $CD8^+$ T cells, promoting their terminal differentiation and functional responses instrumental for tumor rejection. NK/NKT cells would also participate in eliminating tumor cells.

Supplementary references

1. Alexandre YO, Ghilas S, Sanchez C, Le Bon A, Crozat K, Dalod M. XCR1+ dendritic cells promote memory CD8+ T cell recall upon secondary infections with Listeria monocytogenes or certain viruses. *J Exp Med* 2016; **213**: 75-92.
2. Hao Z, Rajewsky K. Homeostasis of peripheral B cells in the absence of B cell influx from the bone marrow. *J Exp Med* 2001; **194**: 1151-1164.
3. Hogquist KA, Jameson SC, Heath WR, Howard JL, Bevan MJ, Carbone FR. T cell receptor antagonist peptides induce positive selection. *Cell* 1994; **76**: 17-27.
4. Schaefer BC, Schaefer ML, Kappler JW, Marrack P, Kedl RM. Observation of antigen-dependent CD8+ T-cell/ dendritic cell interactions in vivo. *Cell Immunol* 2001; **214**: 110-122.
5. Forster R, Schubel A, Breitfeld D*, et al.* CCR7 coordinates the primary immune response by establishing functional microenvironments in secondary lymphoid organs. *Cell* 1999; **99**: 23-33.
6. Muller U, Steinhoff U, Reis LF*, et al.* Functional role of type I and type II interferons in antiviral defense. *Science* 1994; **264**: 1918-1921.
7. Baranek T, Manh TP, Alexandre Y*, et al.* Differential responses of immune cells to type I interferon contribute to host resistance to viral infection. *Cell Host Microbe* 2012; **12**: 571-584.
8. Huang S, Hendriks W, Althage A*, et al.* Immune response in mice that lack the interferon-gamma receptor. *Science* 1993; **259**: 1742-1745.
9. Magram J, Connaughton SE, Warrier RR*, et al.* IL-12-deficient mice are defective in IFN gamma production and type 1 cytokine responses. *Immunity* 1996; **4**: 471-481.
10. Lodolce JP, Boone DL, Chai S*, et al.* IL-15 receptor maintains lymphoid homeostasis by supporting lymphocyte homing and proliferation. *Immunity* 1998; **9**: 669-676.
11. Tomasello E, Naciri K, Chelbi R*, et al.* Molecular dissection of plasmacytoid dendritic cell activation in vivo during a viral infection. *EMBO J* 2018; **37**.
12. Crozat K, Guiton R, Contreras V*, et al.* The XC chemokine receptor 1 is a conserved selective marker of mammalian cells homologous to mouse CD8alpha+ dendritic cells. *J Exp Med* 2010; **207**: 1283-1292.
13. Dorner BG, Dorner MB, Zhou X*, et al.* Selective expression of the chemokine receptor XCR1 on cross-presenting dendritic cells determines cooperation with CD8+ T cells. *Immunity* 2009; **31**: 823-833.
14. Mattiuz R, Wohn C, Ghilas S*, et al.* Novel Cre-Expressing Mouse Strains Permitting to Selectively Track and Edit Type 1 Conventional Dendritic Cells Facilitate Disentangling Their Complexity in vivo. *Front Immunol* 2018; **9**: 2805.
15. Le Bon A, Durand V, Kamphuis E*, et al.* Direct stimulation of T cells by type I IFN enhances the CD8+ T cell response during cross-priming. *J Immunol* 2006; **176**: 4682-4689.
16. Kamphuis E, Junt T, Waibler Z, Forster R, Kalinke U. Type I interferons directly regulate lymphocyte recirculation and cause transient blood lymphopenia. *Blood* 2006; **108**: 3253-3261.
17. Mortier E, Advincula R, Kim L*, et al.* Macrophage- and dendritic-cell-derived interleukin-15 receptor alpha supports homeostasis of distinct CD8+ T cell subsets. *Immunity* 2009; **31**: 811-822.
18. Voehringer D, Liang HE, Locksley RM. Homeostasis and effector function of lymphopenia-induced "memory-like" T cells in constitutively T cell-depleted mice. *J Immunol* 2008; **180**: 4742-4753.
19. Buch T, Heppner FL, Tertilt C*, et al.* A Cre-inducible diphtheria toxin receptor mediates cell lineage ablation after toxin administration. *Nat Methods* 2005; **2**: 419-426.
20. Luche H, Weber O, Nageswara Rao T, Blum C, Fehling HJ. Faithful activation of an extra-bright red fluorescent protein in "knock-in" Cre-reporter mice ideally suited for lineage tracing studies. *Eur J Immunol* 2007; **37**: 43-53.

21. Onami TM, Harrington LE, Williams MA*, et al.* Dynamic regulation of T cell immunity by CD43. *J Immunol* 2002; **168**: 6022-6031.